Published in final edited form as:
Immunity. 2011 October 28; 35(4): 633–646. doi:10.1016/j.immuni.2011.08.016.

Differential Expression of Ly6C and T-bet Distinguish Effector and Memory Th1 CD4+ Cell Properties during Viral Infection

Heather D. Marshall[1,7], **Anmol Chandele**[1,7], **Yong Woo Jung**[1,5], **Hailong Meng**[2], **Amanda C. Poholek**[1], **Ian A. Parish**[1], **Rachel Rutishauser**[1], **Weiguo Cui**[1], **Steven H. Kleinstein**[2,3], **Joe Craft**[1,4], and **Susan M. Kaech**[1,6,*]

[1]Department of Immunobiology, Yale University School of Medicine, New Haven, CT 06520, USA

[2]Department of Pathology, Yale University School of Medicine, New Haven, CT 06520, USA

[3]Interdepartmental Program in Computational Biology and Bioinformatics, Yale University School of Medicine, New Haven, CT 06520, USA

[4]Section of Rheumatology, Department of Internal Medicine, Yale University School of Medicine, New Haven, CT 06520, USA

[5]Department of Pharmacy, Korea University, Chungnam 339-700, Korea

[6]Howard Hughes Medical Institute

SUMMARY

CD4$^+$ T cells differentiate into multiple effector types, but it is unclear how they form memory T cells during infection in vivo. Profiling virus-specific CD4$^+$ T cells revealed that effector cells with T helper 1 (Th1) or T follicular helper (Tfh) cell characteristics differentiated into memory cells, although expression of Tfh cell markers declined over time. In contrast to virus-specific effector CD8$^+$ T cells, increased IL-7R expression was not a reliable marker of CD4$^+$ memory precursor cells. However, decreased Ly6C and T-bet (*Tbx21*) expression distinguished a subset of Th1 cells that displayed greater longevity and proliferative responses to secondary infection. Moreover, the gene expression profile of Ly6C^{lo}T-bet^{int} Th1 effector cells was virtually identical to mature memory CD4$^+$ T cells, indicating early maturation of memory CD4$^+$ T cell features in this subset during acute viral infection. This study provides a framework for memory CD4$^+$ T cell development after acute viral infection.

INTRODUCTION

During acute infections, antigen-specific CD8$^+$ and CD4$^+$ T cells exponentially expand and acquire effector functions to mediate the clearance of pathogens. After the T cell response peaks, the majority of effector cells undergo apoptosis, leaving behind a long-lived population of memory T cells that provides protection upon reinfection. CD8$^+$ T cells primarily differentiate into CTLs, whereas CD4$^+$ T cells can differentiate into a multitude of

*Correspondence: susan.kaech@yale.edu.
[7]These authors contributed equally to this work

ACCESSION NUMBERS

The microarray data are available in the Gene Expression Omnibus (GEO) database (http://www.ncbi.nlm.nih.gov/gds) under accession number GSE32596.

SUPPLEMENTAL INFORMATION

Supplemental Information includes two figures and two tables can be found with this article online at doi:10.1016/j.immuni.2011.08.016.

functionally distinct cell types, such as Th1, Th2, Th17, Tfh, and Treg cells, depending on the type of infection and inflammatory cytokines produced. Our understanding of the mechanisms that control effector and regulatory $CD4^+$ T cell differentiation is much farther advanced than our understanding of how these cells later form memory T cells. Antigen-specific $CD8^+$ T cell memory is remarkably stable in most infections, but whether the same is true for memory $CD4^+$ T cells remains controversial (Homann et al., 2001; MacLeod et al., 2009; Pepper et al., 2010). To date, only a handful of signals have been found to be involved in memory $CD4^+$ T cell development. One critical factor appears to be TCR avidity, because higher avidity interactions enhance survival of antigen-specific $CD4^+$ T cells (Fazilleau et al., 2007; Williams et al., 2008). Additionally, differing strengths of TCR signaling have also been implicated in the cell fate choices between Th1, Th2, and Tfh cells (Blander et al., 2000; Fazilleau et al., 2009; Malherbe et al., 2004). Like $CD8^+$ T cells, persistent exposure to antigen or MHC molecules does not seem necessary for memory $CD4^+$ T cell homeostasis (Purton et al., 2007; Swain et al., 1999). Nevertheless, some studies have suggested that memory $CD4^+$ T cells clonally compete for survival and that continuous MHC class II interactions favorably affect memory $CD4^+$ T cell function (De Riva et al., 2007; Hataye et al., 2006; Polic et al., 2001). Similar to antiviral memory $CD8^+$ T cells, memory $CD4^+$ T cells also require both IL-7 and IL-15 for their long-term survival and homeostasis (Kondrack et al., 2003; Lenz et al., 2004; Li et al., 2003; Purton et al., 2007), but these signals appear less important during effector $CD4^+$ T cell contraction (Tripathi et al., 2007, 2010).

The extensive heterogeneity of $CD4^+$ T cells complicates the study of memory $CD4^+$ T cell formation because the pathways involved may differ according to each cell type. For instance, elegant studies of protein immunizations and viral infections have outlined the formation of heterogenous antigen-specific $CD4^+$ T cell populations that consist of IFN-γ-producing Th1 cells that control viral spread and Tfh cells that migrate to B cell follicles to stimulate antibody production (Fazilleau et al., 2007, 2009; Johnston et al., 2009; Romá n et al., 2002). Therefore, a more complete understanding of memory $CD4^+$ T cell development requires that the different cell types be dissected and their ability to form memory cells examined individually. Doing so will permit investigation of several unresolved questions such as the following. Do all types of effector $CD4^+$ T cells generated during infection possess a similar capacity to differentiate into memory $CD4^+$ T cells, and if so, can memory precursor cells be identified within these populations? What are the genetic pathways and signals utilized to form memory $CD4^+$ T cells and do these differ among the various $CD4^+$ T cell populations? Lastly, are functionally distinct memory $CD4^+$ T cell populations stable over time or do they interconvert at steady state or upon reinfection?

In this study, we sought to distinguish the phenotypically and functionally distinct virus-specific effector $CD4^+$ T cell subsets that form during acute lymphocytic choriomeningitis virus (LCMV) infection and to examine their ability to develop into memory T cells. Most LCMV-specific effector CD4 T cells differentiated into Th1 and Tfh cells as opposed to Treg-, Th2-, or Th17-defined cells, and cells expressing Th1 cell phenotypes populated the memory pool. Cells possessing some, but not all, Tfh cell traits also persisted in the memory CD4 T cell pool. The Th1 cell compartment could be divided into $Ly6C^{hi}T\text{-}bet^{hi}$ and $Ly6C^{lo}T\text{-}bet^{int}$ T cell subsets, and the $Ly6C^{hi}T\text{-}bet^{hi}$ T cell subset produced more IFN-γ and granzyme B (GzmB) relative to the $Ly6C^{lo}T\text{-}bet^{int}$ T cells. T-bet was important for maximal $CD4^+$ T cell expansion and its heightened expression was necessary for formation of $Ly6C^{hi}$ Th1 effector cells. Unlike effector $CD8^+$ T cells, increased IL-7 receptor alpha (IL-7R) expression did not mark memory precursor $CD4^+$ T cells because the $IL\text{-}7R^{lo}$ T cells converted to $IL\text{-}7R^{hi}$ T cells rapidly after viral clearance, and both effector cell subsets gave rise to memory T cells similarly. However, the $Ly6C^{lo}T\text{-}bet^{int}$ Th1 cells had an enhanced ability to persist and proliferate in response to secondary infection compared to the

Ly6C^{hi}T-bet^{hi} T cells. The Ly6C^{lo}T-bet^{int} memory CD4$^+$ T cells also contained CD62L^{hi}CCR7^{hi} central memory T (Tcm) cells. Importantly, the Ly6C^{lo}T-bet^{int} effector CD4$^+$ T cells had a transcriptional signature that was strikingly similar to mature memory CD4$^+$ T cells, indicating that these effector cells attained memory cell features rapidly after infection. Cumulatively, this work provides a molecular and phenotypic foundation for the development of memory Th1 and Tfh cells during a viral infection and identifies phenotypically and functionally distinct subpopulations of virus-specific memory CD4$^+$ T cells that may play different protective roles in long-term immunity to viruses.

RESULTS

Increased IL-7R Expression Does Not Mark Memory Precursor Effector CD4$^+$ T Cells

To begin to study virus-specific memory CD4$^+$ T cells, we first outlined the kinetics of the virus-specific CD4$^+$ T cell response during acute LCMV infection using both GP$_{66–77}$ MHC class II tetramer staining and TCR transgenic Smarta (Stg) CD4$^+$ T cells that recognize the GP$_{66–77}$ epitope of LCMV. The Stg CD4$^+$ T cell response largely reflected the endogenous GP$_{66–77}$-specific CD4$^+$ T cell response in terms of cell number, function, and phenotype (Figure 1A; see Figures S1A and S1B available online). A potential consideration was that GP$_{66–77}$ MHC class II tetramer staining required a 2 hr incubation at 37°C, during which T cells can be activated and certain attributes may be affected (Figure S1B). Therefore, the cross validation of results between the two experimental systems is important for drawing conclusions and was done throughout this study. The Stg and polyclonal GP$_{66–77}$-specific CD4$^+$ T cell response peaked at day 8 postinfection (p.i.) and declined (~10× over 60 days) thereafter, leaving a detectable population of memory CD4$^+$ T cells that was maintained over the time of analysis (~150 days) (Figure 1). Furthermore, LCMV-specific CD4$^+$ T cells were predominantly found in the spleen but could also be recovered from LN, liver, lung, and BM (Figures 1B, 1C, S1C, and S1D).

A major aim of this study was to distinguish the antiviral effector CD4$^+$ T cells that had the greatest ability to persist and populate the memory CD4$^+$ T cell pool. Increased IL-7R expression is a key trait in virus-specific effector CD8$^+$ T cells that helps to distinguish memory precursor cells in some infections (Kaech et al., 2003). The kinetics of IL-7R expression in antiviral CD4$^+$ T cells was similar to that seen in CD8$^+$ T cells; that is, the majority of LCMV-specific effector CD4$^+$ T cells at day 8 p.i. were IL-7R^{lo}, but ~20% of the cells were IL-7R^{hi} (Figures 2A and 2B). Over time as the pool of memory CD4$^+$ T cells formed, the frequency of IL-7R^{hi} T cells increased to comprise more than 90% of the cells (Figures 2A and 2B; Purton et al., 2007). This expression pattern suggested that, like in CD8$^+$ T cells, increased IL-7R expression in CD4$^+$ T cells might also serve as a marker for memory precursor cells. To examine this hypothesis, we first compared whether any of the phenotypes previously found to differ between IL-7R^{hi}CD8$^+$ and IL-7R^{lo}CD8$^+$ T cells, such as expression of T-bet, Bcl-2, and IL-2, were also observed in the CD4$^+$ T cell subsets (Joshi et al., 2007; Kaech et al., 2003). However, unlike CD8$^+$ T cells, the expression of these proteins, and others such as GzmB and IFN-γ, were nearly identical between the IL-7R^{hi} and IL-7R^{lo} effector CD4$^+$ T cells (Figure 2C).

To evaluate directly whether increased IL-7R expression indelibly “marked” effector CD4$^+$ T cells with greater survival and memory cell potential, we sorted day 8 IL-7R^{hi} and IL-7R^{lo} Stg CD4$^+$ T cells and adoptively transferred them into infection-matched congenic recipient mice that were sequentially bled over the next 10 days. This experiment showed that nearly all donor IL-7R^{hi} T cells remained IL-7R^{hi}, but surprisingly, most of the donor IL-7R^{lo} T cells converted into IL-7R^{hi} T cells (Figures 2D and 2E). Therefore, in contrast to antiviral CD8$^+$ T cells, IL-7R was not stably repressed in antiviral CD4$^+$ T cells, and IL-7R^{hi} memory CD4$^+$ T cells arose in part from conversion of IL-7R^{lo} to IL-7R^{hi} effector T cells.

In addition, the absolute number of donor $CD4^+$ T cells recovered after 10 days was nearly identical between the two groups (Figure 2F), and when the recipient mice were infected with LCMV, the secondary expansion of IL-$7R^{hi}$ and IL-$7R^{lo}$ donor $CD4^+$ T cells was quite similar (Figure 2G). Therefore, the survival and secondary proliferative responses of the IL-$7R^{hi}$ and IL-$7R^{lo}$ donor $CD4^+$ T cell populations were comparable. Together, these data show that IL-7R repression is transient in effector $CD4^+$ T cells and is not indicative of cells with shortened lifespan or reduced memory cell potential.

Characterization of Virus-Specific Th1- and Tfh-Containing $CD4^+$ Cell Subsets

Because early differences in IL-7R expression did not help to demarcate effector $CD4^+$ T cells that displayed enhanced survival and memory cell properties, we then investigated whether expression of other relevant T cell markers may distinguish such cells. Our past work on $CD8^+$ T cells identified that T-bet acted as a rheostat in controlling effector $CD8^+$ T cell differentiation. Increased levels of T-bet promoted development of terminal effector $CD8^+$ T cells whereas reduced T-bet expression promoted development of long-lived memory precursor cells (Joshi et al., 2007). Therefore, we investigated whether T-bet expression may similarly distinguish subsets of effector $CD4^+$ T cells with distinct properties and long-term fates. Although decreased IL-7R expression failed to correlate with increased T-bet expression in effector $CD4^+$ T cells (Figure 2C), we found that another receptor regulated by T-bet, Ly6C (Matsuda et al., 2006), could discriminate effector and memory $CD4^+$ T cells that express different amounts of T-bet. $Ly6C^{hi}$ effector $CD4^+$ T cells expressed more T-bet than did $Ly6C^{lo}$ T cells. Interestingly, when Ly6C expression was paired with P-selectin ligand 1 (PSGL1) expression, a receptor that is decreased on Tfh cells (Odegard et al., 2008; Poholek et al., 2010), three distinct subsets of virus-specific $CD4^+$ T cells could be distinguished in direct association with T-bet expression: (1) $PSGL1^{hi}Ly6C^{hi}$ $T\text{-}bet^{hi}$ Th1 cells, (2) $PSGL1^{hi}Ly6C^{lo}T\text{-}bet^{int}$ Th1 cells, and (3) $PSGL1^{lo}Ly6C^{lo}T\text{-}bet^{lo}$ Tfh cells (Figures 3A and S2A). At day 8 p.i, the majority (~50%) of $GP_{66–77}$-specific $CD4^+$ T cells were $PSGL1^{hi}Ly6C^{hi}$ Th1 effector cells that expressed the highest amounts of T-bet, IFN-γ, and GzmB. The second most prevalent subset (~30%) was the $PSGL1^{hi}Ly6C^{lo}$ T effector cells, which also contained Th1 cells, but relative to the $PSGL1^{hi}Ly6C^{hi}$ T cells, expressed intermediate amounts of T-bet and produced modestly less IFN-γ and GzmB. Both $PSGL1^{hi}Ly6C^{hi}$ and $PSGL1^{hi}Ly6C^{lo}$ T cells expressed similar amounts of IL-2, IL-7R, CD122 (IL-2Rβ), and CD27. The third and smallest fraction of the effector cell population (~20%) was the $PSGL1^{lo}$ $Ly6C^{lo}$ T cell subset that contained mostly Tfh cells because they expressed the highest amounts of canonical Tfh cell markers ICOS, CD200, CXCR5, and PD-1 (Figures 3A and S2A). The $PSGL1^{lo}CD4^+$ T cells also expressed the Tfh cell lineage TF *Bcl6* (Figure S2C) and lower amounts of CD27. Interestingly, a substantial portion of the LCMV-specific $CD4^+$ T cells (between 30% and 40% of the cells) did not produce IFN-γ or other trademark Th cell lineage factors including FoxP3 or IL-17, suggesting the existence of additional functioning or less differentiated effector $CD4^+$ T cells (Figures S2D and S2E and data not shown).

Further, we analyzed frozen splenic sections from day 8 LCMV-infected mice by immunofluorescence microscopy to ascertain the location of the $CD4^+$ T cell subsets. Nearly all of the Stg $CD4^+$ T cells sequestered in the B cell follicles were $PSGL1^{lo}$ and $Ly6C^{lo}$ whereas the $PSGL1^{hi}Ly6C^{lo}CD4^+$ T cells were mainly in the T cell zones and the $PSGL1^{hi}Ly6C^{hi}$ T cells localized predominantly to the red pulp (Figures S2F and S2H). Thus, each of these phenotypically and functionally distinct effector subsets occupied discrete anatomical locations in the spleen during a viral infection. Altogether, this analysis showed that at the peak of an acute viral infection, at least three phenotypically, anatomically, and functionally distinct subsets of LCMV-specific effector $CD4^+$ T cells can be identified that vary according to the amount of T-bet expressed.

Tracking the Formation of Th1 and Tfh Memory CD4$^+$ Cells

Next, we followed the different antiviral CD4$^+$ T cell subsets over several months after infection to examine memory cell formation in the spleen, inguinal LN, liver, lung, and BM. $GP_{66–77}$-specific memory CD4$^+$ T cells were found in all tissues examined, but the PSGL1^{lo}CD4$^+$ T cells were found predominantly in the spleen and LNs (Figure S1C). For the most part, the frequencies of three subsets established at the peak of clonal expansion remained fairly consistent; however, there was a noticeable, but insignificant, change in ratio of PSGL1^{hi}Ly6C^{hi} and PSGL1^{hi} Ly6C^{lo} T cells over time (Figures 3C and 3D). At day 8 the Ly6C^{hi} T cells represented ~60% of the PSGL1^{hi} T cell subset, but several months later the Ly6C^{hi} T cells comprised a smaller fraction (~40%) of the population (Figures 3C and 3D). The decline in PSGL1^{hi}Ly6C^{hi} T cells between days 8 and 30 p.i. was even more apparent in the polyclonal CD44^{hi}CD4$^+$ T cell population (Figure 3C, right bar graph).

Next, the phenotypes and functions of the memory CD4$^+$ T cell subsets were examined and, most notably, the hierarchy of T-bet expression was maintained in the three subsets. The PSGL1^{hi}Ly6C^{hi}T-bet^{hi} memory T cells also expressed more IFN-γ and CD122 than their PSLG1^{hi}Ly6C^{lo}T-bet^{int} counterparts. GzmB expression declined rapidly after viral clearance and was not expressed by any of the virus-specific memory CD4$^+$ T cells, and they also expressed similar amounts of IL-7R and CD27 (Figures 3B and S2B). Another noteworthy observation was that in contrast to the phenotypes observed at day 8 p.i, the memory PSGL1^{lo}Ly6C^{lo}CD4$^+$ T cells did not retain high expression of the Tfh cell markers ICOS, CD200, CXCR5, and PD-1 at later time points (compare Figures 3A and 3B). However, the PSGL1^{hi}Ly6C^{lo} and PSGL1^{lo}Ly6C^{lo} T cells maintained slightly higher expression of CXCR5 and ICOS relative to the PSGL1^{hi}Ly6C^{hi} memory T cells. This general reduction in Tfh cell marker expression correlates with the decline in germinal center reactions between 15 and 30 days p.i. and is similar to that previously reported (MacLeod et al., 2011). The PSLG1^{lo}Ly6C^{lo} T cells also maintained lower expression of IFN-γ, IL-2, CD122, and CD27 but expressed similar amounts of IL-7R compared to the PGSL1^{hi} memory T cell subsets. Immunofluorescent microscopy of splenic sections from day 30 p.i. revealed that PSGL1$^+$ T cells remained excluded from B cell follicles after resolution of infection, and the majority of LCMV-specific memory CD4$^+$ T cells were located in the T cell zone and the red pulp (Figure S2G).

Lastly, we analyzed the generation of virus-specific memory CD4$^+$ T cells with Tem and Tcm cell traits. Similar to LCMV-specific CD8$^+$ T cells, CD62L and CCR7 expression is greatly repressed on the virus-specific effector CD4$^+$ T cells early during infection, but over time CD62L$^+$CCR7$^+$ Tcm cells gradually emerged in the memory CD4$^+$ T cell population (Figure 3E). Interestingly, when combined with Ly6C, we found that the CD62L$^+$CCR7$^+$ Tcm cells were preferentially, but not exclusively, enriched in the Ly6C^{lo} memory T cell compartment compared to the Ly6C^{hi} T cell compartment. Collectively, these data show that after acute LCMV infection, the memory CD4$^+$ T cell population is heterogeneous and functionally diverse. IFN-γ-producing Th1 memory CD4$^+$ cells persist, but there is a general reduction of Tfh cell-associated markers in the resting memory CD4$^+$ T cell pool. Over time, the PSGL1^{hi}Ly6C^{lo} memory CD4$^+$ T cell population becomes the dominant subset and contains Tcm cells.

T-bet-Dependent Regulation of Virus-Specific Effector CD4$^+$ T Cell Subsets

To better understand the factors that control the development of these functionally diverse effector CD4$^+$ T cell subsets, we interrogated the role of T-bet because it was expressed in a graded manner in the three virus-specific CD4$^+$ T cell subsets. We examined the effect of removing one or two copies of *Tbx21* on the types of virus-specific CD4$^+$ T cells that form by generating an allelic series of *Tbx21*$^{+/+}$, *Tbx21*$^{+/-}$, and *Tbx21*$^{-/-}$ Stg TCR transgenic

mice to use as donor cells for chimeras. Eight days after LCMV infection, the functional and phenotypic characteristics of the Stg $CD4^+$ T cells were analyzed. As expected given its role in Th1 cell lineage commitment, we observed a dose-dependent reduction in the percentage of IFN-γ-producing Th1 cells in the *Tbx21*$^{+/-}$ and *Tbx21*$^{-/-}$ Stg $CD4^+$ T cells (data not shown). Additionally, similar to LCMV-specific $CD8^+$ T cells, we saw a strong requirement for T-bet for maximal clonal expansion of virus-specific $CD4^+$ T cells (Figure 4; Joshi et al., 2007). Most notably, we examined the types of effector $CD4^+$ T cells that formed and found that the frequency of $PSGL1^{hi}Ly6C^{hi}$ T cells directly correlated with *Tbx21* gene copy number. Removal of one (*Tbx21*$^{+/-}$) or two (*Tbx21*$^{-/-}$) copies of the gene encoding T-bet decreased the proportion of $PSGL1^{hi}Ly6C^{hi}$ effector $CD4^+$ T cells that formed by ~30% and ~50%, respectively (Figure 4). Likewise, there was dose-dependent compensatory increase in the fraction of $PSGL1^{hi}Ly6C^{lo}$ and $PSGL1^{lo}Ly6C^{lo}$ effector $CD4^+$ T cells. Thus, T-bet deficiency most overtly affected the formation of $PSGL1^{hi}Ly6C^{hi}$ Th1 cells, in accordance with its increased abundance in this subset. These results demonstrate that T-bet acts in a graded manner to generate functionally diverse effector $CD4^+$ T cell subsets during viral infection.

$PSGL1^{hi}Ly6C^{lo}CD4^+$ T Cells Display Enhanced Survival and Proliferative Responses to Reinfection

The above comparisons revealed several interesting parallels between $CD4^+$ and $CD8^+$ effector and memory T cell differentiation during LCMV infection. For instance, $KLRG1^{lo}IL\text{-}7R^{hi}$ memory precursor $CD8^+$ T cells (1) express less T-bet, (2) preferentially localize to the T cell zone, (3) have greater longevity, (4) give rise to self-renewing Tcm cells at resting states, and (5) mount stronger proliferative responses after secondary infection than $KLRG1^{hi}IL\text{-}7R^{lo}$ short-lived effector T cells (Joshi et al., 2007; Jung et al., 2010; Kaech et al., 2003). Likewise, the $PSGL1^{hi}Ly6C^{lo}CD4^+$ T cells similarly expressed less T-bet, preferentially localized to the T cell zone, contained Tcm cells, and constituted a greater proportion of the memory $CD4^+$ T cell population. Therefore, we hypothesized that the $PSGL1^{hi}Ly6C^{lo}$ T cell subset may contain less differentiated Th1 cells with additional memory cell features.

To investigate this point more closely, we compared two cardinal memory T cell properties between the $PSGL1^{hi}Ly6C^{hi}$ and $PSGL1^{hi}Ly6C^{lo}$ effector $CD4^+$ T cell subsets: enhanced survival during the contraction phase and proliferative responses to secondary infection. First, to determine whether there were differences in the ability of the effector subsets to persist after viral clearance, we purified $PSGL1^{hi}Ly6C^{hi}$ and $PSGL1^{hi}Ly6C^{lo}$ Stg effector $CD4^+$ T cells at day 8 p.i. and transferred equal cell numbers into separate groups of uninfected congenically marked recipient mice. After 7–10 days, we observed that a substantially larger number of $Ly6C^{lo}$ donor T cells were recovered in the spleen and other tissues relative to the $Ly6C^{hi}$ donor T cells (Figure 5A and data not shown), indicating that the $Ly6C^{lo}$ effector $CD4^+$ T cells were preferentially maintained during the contraction phase relative to their $Ly6C^{hi}$ T cell counterparts. We then examined the phenotypic stability of the donor cells and found that most $Ly6C^{hi}$ donor T cells remained $Ly6C^{hi}$, but ~50% of the $Ly6C^{lo}$ T cells became $Ly6C^{hi}$ after transfer (Figure 5A, right). Further, the hierarchy of T-bet expression was dictated by the current phenotype of the cells and not the donor phenotype; that is, $Ly6C^{lo}$ donor T cells that converted to $Ly6C^{hi}$ T cells expressed more T-bet than $Ly6C^{lo}$ T cells that maintained their $Ly6C^{lo}$ phenotype (data not shown). Together, these observations demonstrate that the $Ly6C^{hi}$ effector $CD4^+$ T cells did not persist as well as the $Ly6C^{lo}$ T cells and suggest that increased Ly6C expression may be a terminal phenotypic marker of Th1 $CD4^+$ cells. That $Ly6C^{lo}T\text{-}bet^{int}$ T cells converted to $Ly6C^{hi}T\text{-}bet^{hi}$ T cells after transfer, in the absence of further antigenic stimulation, also suggested an interesting model of memory $CD4^+$ T cell homeostasis whereby the $Ly6C^{lo}CD4^+$ T cells

steadily repopulate and sustain the pool of $Ly6C^{hi}$ Tem memory $CD4^+$ cells. This model helps to explain the existence of $Ly6C^{hi}CD4^+$ T cells at all time points examined (Figure 3C). Therefore, the greatest ability to survive the contraction phase and the plasticity to further differentiate into terminal Th1 effector cells resides within the effector $Ly6C^{lo}CD4^+$ T cell population.

Next, we compared the ability of the $PSGL1^{hi}Ly6C^{hi}$ and $PSGL1^{hi}Ly6C^{lo}$ memory $CD4^+$ T cells isolated from days 30–60 after LCMV infection to respond to a secondary infection by transferring equal numbers of donor Stg $CD4^+$ T cells from each subset and infecting the recipient mice 1 day later with LCMV clone 13. These experiments showed that the memory $Ly6C^{lo}$ T cells possessed a greater ability to undergo secondary proliferation compared to the $Ly6C^{hi}$ T cells (Figure 5B). As expected based on a linear model of differentiation, after secondary infection the majority of the donor $Ly6C^{hi}CD4^+$ T cells remained $Ly6C^{hi}$, whereas more than half of the $Ly6C^{lo}$ T cells became $Ly6C^{hi}$ secondary effector T cells (Figure 5B, right). When these experiments were repeated with donor $PSGL1^{hi}Ly6C^{hi}$ and $PSGL1^{hi}Ly6C^{lo}$ effector $CD4^+$ T cells from day 8 p.i., nearly identical results to the donor memory T cells were observed. That is, the day 8 $Ly6C^{lo}$ effector $CD4^+$ T cells also displayed a more robust secondary burst than the $Ly6C^{hi}$ donor T cells and many cells upregulated Ly6C expression (Figure 5C). Collectively, this series of experiments demonstrated that two key memory cell properties (increased survival during the contraction phase and the ability to robustly proliferate upon secondary infection) were enhanced in virus-specific $Ly6C^{lo}CD4^+$ T cells. These traits were evident as early as day 8 p.i., suggesting that the $PSGL1^{hi}Ly6C^{hi}$T-bet^{hi} T cell subset contained more terminally differentiated Th1 cells whereas the $PSGL1^{hi}Ly6C^{lo}$T-bet^{int} T cell subset contained less differentiated Th1 cells that displayed a greater capacity to persist and respond to secondary infection.

Transcriptional Profile of $PSGL1^{hi}Ly6C^{lo}$ Effector $CD4^+$ T Cells Resembles Memory $CD4^+$ T Cells

To further characterize the effector subsets and identify genetic pathways and transcription factors involved in their differentiation, we performed genome-wide gene expression profiling of the three day 8 effector cell populations: (1) $PSGL1^{hi}Ly6C^{hi}$, (2) $PSGL1^{hi}Ly6C^{lo}$, and (3) $PSGL1^{lo}Ly6C^{lo}$, along with (4) day 60 memory $PSGL1^{hi}$ and (5) naive Stg $CD4^+$ T cells via Illumina BeadChips. Results of this microarray confirmed the validity of our phenotyping by flow cytometry in many ways and showed distinct gene signatures for the three effector subsets. For example, the $PSGL1^{lo}Ly6C^{lo}$ T cell subset showed increased expression of Tfh cell signature genes such as *Cxcr5*, *Pdcd1* (PD1), *Il21* (IL-21), and *Bcl6* (Figure 6A, green asterisks; Table S1). The $PSGL1^{hi}Ly6C^{hi}$ effector $CD4^+$ T cells were more Th1 cell-like with increased expression of *Tbx21*, *Ifng*, and *Cxcr3* (Figure 6A, red asterisks; Table S1). The $PSGL1^{hi}Ly6C^{lo}$ effector $CD4^+$ T cells also displayed increased expression of Th1 cell genes, but these were expressed at relatively lower levels than their $Ly6C^{hi}$ T cell counterparts (Figure 6A; Table S1).

Clustering analysis was performed on signature gene sets containing genes differentially expressed by at least 32-fold in any one group relative to naive Stg $CD4^+$ T cells, and a heatmap of these expression values was generated. This analysis revealed an unexpected finding in that the day 8 $PSGL1^{hi}Ly6C^{lo}$ T cells clustered more closely with day 60 memory cells than their day 8 $PSGL1^{hi}Ly6C^{hi}$ effector $CD4^+$ T cell counterparts (Figure 6A). The same relationship was also found when considering a 2-fold cutoff or when considering the set of most variable genes across the samples (CV > 0.5) (data not shown). We also performed a pair-wise comparison of the differentially expressed genes between all the different groups relative to naive $CD4^+$ T cells (greater than 2-fold change and $q < 0.05$), and this again revealed a striking correlation ($r = 0.95$) in the gene expression patterns

between day 8 PSGL1^{hi}Ly6C^{lo} effector T cells and day 60 PSGL1^{hi} memory CD4^{+} T cells (Figure 6B). Similarity in gene expression between the two day 8 PSGL1^{hi}Ly6C^{lo} and PSGL1^{hi}Ly6C^{hi} effector T cell populations was also evident ($r = 0.85$) but considerably less than the day 60 memory CD4^{+} T cells, and less similarity in gene expression was observed between day 60 PSGL1^{hi} memory T cells and either day 8 PSGL1^{hi}Ly6C^{hi} ($r = 0.78$) or PSGL1^{lo}Ly6C^{lo} ($r = 0.78$) effector T cells. Thus, even by day 8 p.i., the PSGL1^{hi}Ly6C^{lo} T cells displayed a gene expression profile that was nearly identical to mature memory CD4^{+} T cells. These data suggest that the Ly6C^{lo} effector T cells started to acquire memory CD4^{+} T cell qualities early after infection, which may be akin to the rapid transition of effector CD4^{+} T cells to mature memory cells after removal of antigen previously reported (McKinstry et al., 2007).

Finally, we directly compared the gene expression profiles of PSGL1^{hi}Ly6C^{hi} and PSGL1^{hi}Ly6C^{lo} effector Th1 CD4^{+} cells. Surprisingly, this revealed the presence of several Treg cell-associated genes such as *Foxp3*, *Cd83*, *Nt5e* (CD73), *Itgae* (CD103), and *Folr4* in the Ly6C^{lo} T cell subset, despite not detecting FoxP3^{+} GP$_{66–77}$-specific CD4^{+} T cells by intracellular staining (Table 1; Figure S2D). Other notable differences between these Ly6C^{hi} and Ly6C^{lo} T cell subsets were receptors involved in migration and adhesion such as *Ccr7*, *Cx3cr1*, *Ccr6*, *Sell* (CD62L), the integrins *Itgae* (CD103) and *Itgad* (CD11d), and potential survival factors *Il6ra*, *Serpina3g* (Spi2a), and *Igf1r*. For additional details on the differentially expressed genes across the different cell populations including transcription factors, cytokines, chemokines, and cytokine/chemokine receptors, refer to Table S2. In summary, these data identify numerous candidate genes that could contribute to differential functions and fates of the distinct effector CD4^{+} T cell subsets and the enhanced memory cell potential of Ly6C^{lo} effector T cells.

DISCUSSION

Despite the indispensable role of CD4^{+} T cells in the preservation of long-term immunity to pathogens, the factors regulating the survival of effector CD4^{+} T cells and their transition to memory CD4^{+} T cells are largely unknown. Because CD4^{+} T cells can differentiate into numerous functionally distinct populations of helper T cells during infection, it is imperative that one first dissects and examines memory cell formation in each effector cell subset individually to gain a clearer understanding of memory CD4^{+} T cell development. In this study we performed a comprehensive phenotypic, functional, and genomic profiling of LCMV-specific CD4^{+} T cells during their effector to memory transition. Our study revealed that during LCMV infection, virus-specific CD4^{+} T cells differentiated into Th1 and Tfh effector cells that could be distinguished by differential expression of PSGL1 and Ly6C. Cells containing Th1 and Tfh cell features were present in the resting memory pool, but interestingly, most markers commonly used to define Tfh cells (such as increased expression of PD1, CXCR5, ICOS, and CD200) decreased over time on the PSGL1^{lo} memory CD4^{+} T cells. Two major subsets of antiviral Th1 cells could be distinguished based on expression of Ly6C, a GPI-anchored membrane glycoprotein with poorly defined function that can act as a costimulatory molecule for T cells (Bamezai, 2004). We propose that the Ly6C^{hi} effector CD4^{+} T cells represent more terminally differentiated Th1 cells because they expressed greater amounts of T-bet, CD122, IFN-γ, and GzmB and had increased rates of contraction and reduced proliferative responses relative to the Ly6C^{lo} T cells. Furthermore, the Ly6C^{lo} Th1 effector cells displayed a gene expression profile strikingly similar to that of mature memory CD4^{+} T cells and contained Tcm cells. It will be important in the future to examine how these phenotypically and functionally distinct Th1 cell subsets vary across different types of infections and immunizations, especially in cases where CD4^{+} T cell memory decays over time.

This study identifies several interesting differences and parallels with memory $CD8^+$ T cell development. Increased IL-7R expression identifies effector $CD8^+$ T cells (IL-$7R^{hi}$ CTLs) with increased memory cell potential (Kaech et al., 2003). Based on the similar IL-7R expression patterns between LCMV-specific $CD4^+$ and $CD8^+$ T cells, we predicted that differential IL-7R expression might also distinguish short- and long-lived effector $CD4^+$ T cells. However, a different scenario was revealed in which the IL-7R repression was transient in $CD4^+$ T cells and the IL-$7R^{lo}$ effector T cells converted to IL-$7R^{hi}$ cells. Both IL-$7R^{hi}CD4^+$ and IL-$7R^{lo}CD4^+$ T cells showed an equal ability to survive and populate the memory $CD4^+$ T cell pool and had comparable responses to secondary infection. Thus, decreased IL-7R expression was not a defining feature of short-lived effector $CD4^+$ T cells. The difference in the stability of IL-7R repression between effector $CD4^+$ and $CD8^+$ T cells may be due to variations in the transcriptional repressor Gfi-1 that can repress *Il7ra* transcription in $CD8^+$ but not in $CD4^+$ T cells (Chandele et al., 2008; Park et al., 2004). However, despite this important difference between virus-specific $CD4^+$ and $CD8^+$ T cells, this study revealed other noteworthy conceptual and functional similarities between $Ly6C^{lo}CD4^+$ Th1 cells and IL-$7R^{hi}CD8^+$ CTL. For instance, with respect to the $Ly6C^{hi}$ Th1 and IL-$7R^{lo}$ CTL cells, the $Ly6C^{lo}$ Th1 and IL-$7R^{hi}$ CTL cells displayed enhanced survival during the contraction phase and greater proliferative responses to secondary infection. The $Ly6C^{lo}$ Th1 cells and IL-$7R^{hi}$ CTL also preferentially resided in the T cell zone whereas the $Ly6C^{hi}$ Th1 cells and IL-$7R^{lo}$ CTL predominantly localized to the red pulp in the spleen. Additionally, both the $Ly6C^{lo}$ memory $CD4^+$ T cell and IL-$7R^{hi}CD8^+$ T cell populations contained a greater frequency of $CD62L^+CCR7^+$ Tcm cells compared to the $Ly6C^{hi}CD4^+$ and IL-$7R^{lo}CD8^+$ T cells (Kaech et al., 2003).

Lastly, the graded expression of T-bet was observed in both effector $CD4^+$ and $CD8^+$ T cell subsets with the $Ly6C^{hi}$ Th1 cells and IL-$7R^{lo}$ CTL expressing higher amounts of T-bet compared to the $Ly6C^{lo}$ Th1 cells and IL-$7R^{hi}$ CTL. In both T cell types, elevated amounts of T-bet were required for maximal clonal expansion and formation of terminal $PSGL1^{hi}Ly6C^{hi}$ Th1 cells and IL-$7R^{lo}$ CTL, and likewise, reducing T-bet by one or two copies proportionally increased the frequency of $PSGL1^{hi}Ly6C^{lo}$ Th1 cells and IL-$7R^{hi}$ CTL (Joshi et al., 2007). Thus, T-bet acts in a dose-dependent manner in both $CD4^+$ and $CD8^+$ T cells to generate distinct effector cell subpopulations, and we propose that, analogous to $CD8^+$ T cells, T-bet may act like a rheostat during Th1 cell differentiation to balance terminal effector cell differentiation and memory cell potential. Additionally, one may consider the $Ly6C^{lo}$ Th1 cells and IL-$7R^{hi}$ CTL to be more plastic or multipotent because these cells can develop into $Ly6C^{hi}$ T-bet^{hi} Th1 cells and IL-$7R^{lo}$T-bet^{hi} CTL, respectively, upon re-stimulation whereas the converse was not as evident. These data suggest a linear model of effector differentiation common to $CD4^+$ and $CD8^+$ T cells wherein “less differentiated” T-bet^{int} effector cells can form and persist or further differentiate into terminal T-bet^{hi} effector cells with robust effector function but reduced memory cell potential. Identifying the signals that direct the development of $Ly6C^{hi}$T-bet^{hi} and $Ly6C^{lo}$T-bet^{int} Th1 cells and whether Ly6C itself is involved in this process will be important to address in the future.

In agreement with previous work (Harrington et al., 2008; Pepper et al., 2010), our data showed that LCMV-specific Th1 cells efficiently entered the memory pool. However, our work also showed that not all Th1 cells have an equal potential to do so because the $PSGL1^{hi}Ly6C^{lo}$T-bet^{int} effector $CD4^+$ T cells showed greater rates of persistence and accumulation in the memory cell pool after infection. Our gene expression profiling between $PSGL1^{hi}Ly6C^{hi}$ and $PSGL1^{hi}Ly6C^{lo}$ effector T cells identified several differentially expressed candidate genes that could potentially increase the lifespan of $PSGL1^{hi}Ly6C^{lo}$ T cells such as *Serping3a* (Spi2a), *Il6ra*, and *Igf1r*. Interestingly, Spi2a is also elevated in $CD8^+$ memory precursor cells and is necessary for memory $CD8^+$ T cell formation (Liu et

al., 2004). Nonetheless, at all time points examined, ~30%–40% of the memory $CD4^+$ T cell population contained $PSGL1^{hi}Ly6C^{hi}$ T cells. Interestingly, the results of our adoptive transfer experiments showed that interconversion between the subsets was occurring even in the absence of antigen restimulation. The conversion from $Ly6C^{lo}$ to $Ly6C^{hi}$ Th1 cells was greatest, suggesting that the $Ly6C^{hi}$ memory $CD4^+$ T cell compartment is homeostatically replenished from $Ly6C^{lo}$ memory T cells. It is currently unclear what drives $Ly6C^{lo} \rightarrow Ly6C^{hi}$ $CD4^+$ T cell conversion in the absence of antigen, but one candidate is type I IFNs because these can induce Ly6C expression in T cells (Khan et al., 1990). Therefore, bystander exposure to inflammatory cytokines may impact $CD4^+$ memory T cell phenotype, function, and homeostasis. On this note, another report also showed that memory $CD4^+$ T cells generated by a noninfectious immunization (peptide + LPS) preferentially reside in the BM and express Ly6C (Tokoyoda et al., 2009); however, our study on viral infection and that previously on bacterial infection (Pepper et al., 2010) did not reveal a similar tissue tropism. LCMV-specific $CD4^+$ T cells did reside in the BM, but the frequency and number was less than that observed in the spleen and liver and comparable to that in LN and lung.

Our data also show that LCMV-specific $PSGL1^{lo}Ly6C^{lo}CD4^+$ T cells were present at memory time points, even after germinal center responses had ceased, but these $PSGL1^{lo}Ly6C^{lo}$ memory T cells did not sustain expression of the other canonical Tfh cell markers. Based on prior studies that demonstrated $CXCR5^+$ memory $CD4^+$ T cells could “help” secondary B cell responses (Fazilleau et al., 2007; MacLeod et al., 2011), our data would suggest that the $PSGL1^{lo}Ly6C^{lo}$ (and possibly some $PSGL1^{hi}Ly6C^{lo}$) memory $CD4^+$ T cells contain “rested down” Tfh memory cells, but this requires further investigation.

Although most LCMV-specific $CD4^+$ T cells developed into Th1 cells that produced IFN-γ, a substantial fraction (~30%–40%) of the cells did not produce IFN-γ and this is consistent with previous reports (Harrington et al., 2008; Johnston et al., 2009). Furthermore, our analysis indicated they did not produce substantial amounts of other signature effector T cell cytokines (IL-17, IL-5, or IL-13) or express high amounts of FoxP3. This observation suggests that some antiviral $CD4^+$ T cells exist in an uncommitted or less differentiated state, or alternatively, perform functions that remain to be discovered. Moreover, it was not surprising to find increased abundance of mRNAs for the TFs *Tbx21* and *Eomes*, the cytokines *Ifng*, *Il18*, and *Il2*, the cytokine receptors *IL2rb*, *IL12rb1*, *IL18r1*, and *IL18rap,* and the chemokine receptors *Ccr5* and *Cxcr3* in $PSGL1^{hi}$ memory $CD4^+$ T cells relative to naive $CD4^+$ T cells given their Th1 cell developmental bias. But an unexpected observation that emerged was that the memory $CD4^+$ T cells also contained elevated amounts of mRNAs of other $CD4^+$ Th cell lineage-determining TFs (*Foxp3*, *c-maf*, *Rorc*, *Rora*), cytokines (*Il21*, *Il10*, and *Il4*), cytokine receptors (*Illr2*, *IL10ra*, *IL17rb*, and *IL17re*), and chemokine receptors (*Ccr6*, *Ccr4*, and *Cxcr5*) relative to naive T cells. These data point to the possibility that memory $CD4^+$ T cells exist in a polyfunctional poised state and may be responsive to a multitude of cytokines that could influence their form and function during subsequent infections. Perhaps memory $CD4^+$ T cells embody significant plasticity that permits inter-conversion or transdifferentiation between functionally distinct populations of $CD4^+$ T cells as has been recently reported (O’Shea and Paul, 2010). Further studies examining the plasticity of antigen-specific Tfh and Th1 cell-containing memory $CD4^+$ populations will determine whether their identities are stably maintained or whether conversion occurs between $CD4^+$ memory subsets after reinfection. Understanding the molecular mechanisms of memory $CD4^+$ T cell generation, maintenance, and plasticity will have biological implications for designing therapeutic vaccination regimes against infections.

EXPERIMENTAL PROCEDURES

Mice and Infections

C57BL/6Ncr mice were purchased from the National Cancer Institute (Frederick, MD). Stg chimeric mice were generated by adoptive transfer of ~1 × 10^4 Thy1.1$^+$ Stg CD4$^+$ T cells into naive Thy1.2$^+$ C57BL/6 mice and rested for at least 1 day before infection. *Tbx21*$^{-/-}$ mice were obtained from L. Glimcher (Harvard Medical School, Cambridge, MA) and crossed to Stg TCR transgenic mice. Mice were infected i.p. with 2 × 10^5 pfu LCMV Armstrong or 2 × 10^6 pfu LCMV clone 13. All animal experiments were done with approved Institutional Animal Care and Use Committee protocols.

Antibodies for Surface and Intracellular Staining

Lymphocyte isolation and surface and intracellular staining was performed as described previously (Joshi et al., 2007). For in vitro stimulation, CD4$^+$ T cells were stimulated with the $GP_{61–80}$ peptide (1 μg/ml) for 6 hr with Brefeldin A. $GP_{66–77}$ MHC class II tetramer (NIH tetramer core facility, Emory University, Atlanta, GA) staining was performed as described (Johnston et al., 2009). Antibodies were purchased from Ebioscience (San Diego, CA), BD PharMingen (San Diego, CA), or BioLegend (San Diego, CA). Flow cytometry was acquired on BD LSRII with Diva software and analyzed with Flow Jo software (Treestar, San Carlos, CA).

Cell Isolation and Adoptive Transfers

Splenocytes were isolated from indicated days p.i. as previously described (Joshi et al., 2007), enriched via negative selection or positive selection with FlowComp mouse CD4$^+$ Dynabeads (Invitrogen, Carlsbad, CA), stained with requisite antibodies, and sorted with a FACSAria (BD Biosciences). Equal numbers of Thy1.1$^+$IL-7R^{hi} and Thy1.1$^+$IL-7R^{lo} T cells or Thy1.1$^+$PSGL1^{hi} Ly6C^{hi} and Thy1.1$^+$PSGL1^{hi}Ly6C^{lo} T cells were transferred i.v. to either naive or infection-matched (Thy1.2) recipient mice i.v. and analyzed at indicated time points posttransfer. For recall experiments, mice were infected 1 or 30 days after adoptive transfer with 2 × 10^6 pfu LCMV clone 13.

Immunofluorescent Microscopy

On day 8 or day 30 after LCMV infection, spleens were isolated and embedded in OCT compound (Sakura). Tissue blocks were frozen in isopentane (Sigma-Aldrich) chilled by dry ice. Eight micrometer sections were cut with a cryostat, air-dried, and fixed with cold acetone. Sections were stained with 1–5 μg/ml mAb against B220, CD4, F4/80, PSGL1, Ly6C, Ly5.2, and/or Thy1.1. The biotinylated Abs were visualized with Alexa 568-conjugated streptavidin (Invitrogen). Images were captured on an Olympus BX-40 microscope with a SPOT-RT Slider (Scanalytics) digital camera.

Gene Expression Profiling and qRT-PCR

DNA microarray analysis was performed on three independent samples of five different Stg CD4$^+$ T cell populations (purified to >95% purity on FACSAria [BD Biosciences]): (1) naive, (2) day 8 PSGL1^{lo}, (3) day 8 PSGL1^{hi}Ly6C^{hi}, (4) day 8 PSGL1^{hi}Ly6C^{lo}, and (5) day 60 PSGL1^{hi} memory T cells. RNA was isolated with RNeasy kits (QIAGEN, Valencia, CA) and was hybridized to MouseRef-6 Bead-Chips (Illumina, San Diego, CA) at the Yale Keck Microarray Facility. The micro-array analysis was carried out with packages in R (R Development CoreTeam, 2010). Raw microarray data were normalized with the quantile method provided by the lumi package. Differential gene expression was defined by two criteria: (1) an absolute fold-change ≥2 relative to naive samples and (2) a statistically significant change in expression as determined by LIMMA with a Benjamani-Hochberg

false discovery rate cutoff $q < 0.05$. Heatmaps were generated with a fold-change ≥ 32 and $q < 0.0001$. Hierarchical clustering was based on Euclidean distance metric and Ward's linkage. In addition, the microarray data were also analyzed with GeneSpring GX 11.5.1 (Agilent Technologies) with quantile normalization. Gene lists for Table 1 and Tables S1 and S2 were generated on the basis of fold changes from this analysis along with consideration of biological relevance.

qRT-PCR was performed as previously described (Chandele et al., 2008) and values were normalized to the ribosomal protein L9. Primers used were as follows: *L9*: 5′-TGAAGAAATCTGTGGGTCG-3′ (forward), 5′-GCACTACGG ACATAGGAACT-3′ (reverse); *Tbx21*: 5′-CAACAACCCCT TTGCCAAAG-3′ (forward), 5′-TCCCCCAA GCAGTTGACAGT-3′ (reverse); *Bcl6*: 5′-CTGCAG ATGGAGCATGTTGT-3′ (forward), 5′-CACCCGGGAGTATTTCTCAG-3′.

Statistical Analysis

Where indicated, p values were determined by two-tailed unpaired Student's t test. p values < 0.05 were considered significant. All error bars represent standard deviation.

Supplementary Material

Refer to Web version on PubMed Central for supplementary material.

Acknowledgments

The authors would like to thank C. Dominguez, C. Perry, and other members of the S.M.K. and J.C. labs for helpful comments and technical expertise. We also thank M. Shlomchik for use of his fluorescent microscope and H. Hengartner for Stg transgenic mice supplied by R. Ahmed. This work was supported by NIH RO1 AI074699 (S.M.K.) and NIH AI07019 (H.D.M.).

References

Bamezai A. Mouse Ly-6 proteins and their extended family: markers of cell differentiation and regulators of cell signaling. Arch Immunol Ther Exp (Warsz). 2004; 52:255–266. [PubMed: 15467490]

Blander JM, Sant'Angelo DB, Bottomly K, Janeway CA Jr. Alteration at a single amino acid residue in the T cell receptor alpha chain complementarity determining region 2 changes the differentiation of naive CD4 T cells in response to antigen from T helper cell type 1 (Th1) to Th2. J Exp Med. 2000; 191:2065–2074. [PubMed: 10859331]

Chandele A, Joshi NS, Zhu J, Paul WE, Leonard WJ, Kaech SM. Formation of IL-7Ralphahigh and IL-7Ralphalow CD8 T cells during infection is regulated by the opposing functions of GABPalpha and Gfi-1. J Immunol. 2008; 180:5309–5319. [PubMed: 18390712]

De Riva A, Bourgeois C, Kassiotis G, Stockinger B. Noncognate interaction with MHC class II molecules is essential for maintenance of T cell metabolism to establish optimal memory CD4 T cell function. J Immunol. 2007; 178:5488–5495. [PubMed: 17442930]

Fazilleau N, Eisenbraun MD, Malherbe L, Ebright JN, Pogue-Caley RR, McHeyzer-Williams LJ, McHeyzer-Williams MG. Lymphoid reservoirs of antigen-specific memory T helper cells. Nat Immunol. 2007; 8:753–761. [PubMed: 17529982]

Fazilleau N, McHeyzer-Williams LJ, Rosen H, McHeyzer-Williams MG. The function of follicular helper T cells is regulated by the strength of T cell antigen receptor binding. Nat Immunol. 2009; 10:375–384. [PubMed: 19252493]

Harrington LE, Janowski KM, Oliver JR, Zajac AJ, Weaver CT. Memory CD4 T cells emerge from effector T-cell progenitors. Nature. 2008; 452:356–360. [PubMed: 18322463]

Hataye J, Moon JJ, Khoruts A, Reilly C, Jenkins MK. Naive and memory CD4+ T cell survival controlled by clonal abundance. Science. 2006; 312:114–116. [PubMed: 16513943]

Homann D, Teyton L, Oldstone MB. Differential regulation of antiviral T-cell immunity results in stable CD8+ but declining CD4+ T-cell memory. Nat Med. 2001; 7:913–919. [PubMed: 11479623]

Johnston RJ, Poholek AC, DiToro D, Yusuf I, Eto D, Barnett B, Dent AL, Craft J, Crotty S. Bcl6 and Blimp-1 are reciprocal and antagonistic regulators of T follicular helper cell differentiation. Science. 2009; 325:1006–1010. [PubMed: 19608860]

Joshi NS, Cui W, Chandele A, Lee HK, Urso DR, Hagman J, Gapin L, Kaech SM. Inflammation directs memory precursor and short-lived effector CD8(+) T cell fates via the graded expression of T-bet transcription factor. Immunity. 2007; 27:281–295. [PubMed: 17723218]

Jung YW, Rutishauser RL, Joshi NS, Haberman AM, Kaech SM. Differential localization of effector and memory CD8 T cell subsets in lymphoid organs during acute viral infection. J Immunol. 2010; 185:5315–5325. [PubMed: 20921525]

Kaech SM, Tan JT, Wherry EJ, Konieczny BT, Surh CD, Ahmed R. Selective expression of the interleukin 7 receptor identifies effector CD8 T cells that give rise to long-lived memory cells. Nat Immunol. 2003; 4:1191–1198. [PubMed: 14625547]

Khan KD, Lindwall G, Maher SE, Bothwell AL. Characterization of promoter elements of an interferon-inducible Ly-6E/A differentiation antigen, which is expressed on activated T cells and hematopoietic stem cells. Mol Cell Biol. 1990; 10:5150–5159. [PubMed: 1697928]

Kondrack RM, Harbertson J, Tan JT, McBreen ME, Surh CD, Bradley LM. Interleukin 7 regulates the survival and generation of memory CD4 cells. J Exp Med. 2003; 198:1797–1806. [PubMed: 14662907]

Lenz DC, Kurz SK, Lemmens E, Schoenberger SP, Sprent J, Oldstone MB, Homann D. IL-7 regulates basal homeostatic proliferation of antiviral CD4+T cell memory. Proc Natl Acad Sci USA. 2004; 101:9357–9362. [PubMed: 15197277]

Li J, Huston G, Swain SL. IL-7 promotes the transition of CD4 effectors to persistent memory cells. J Exp Med. 2003; 198:1807–1815. [PubMed: 14676295]

Liu N, Phillips T, Zhang M, Wang Y, Opferman JT, Shah R, Ashton-Rickardt PG. Serine protease inhibitor 2A is a protective factor for memory T cell development. Nat Immunol. 2004; 5:919–926. [PubMed: 15311278]

MacLeod MK, Clambey ET, Kappler JW, Marrack P. CD4 memory T cells: what are they and what can they do? Semin Immunol. 2009; 21:53–61. [PubMed: 19269850]

MacLeod MK, David A, McKee AS, Crawford F, Kappler JW, Marrack P. Memory CD4 T cells that express CXCR5 provide accelerated help to B cells. J Immunol. 2011; 186:2889–2896. [PubMed: 21270407]

Malherbe L, Hausl C, Teyton L, McHeyzer-Williams MG. Clonal selection of helper T cells is determined by an affinity threshold with no further skewing of TCR binding properties. Immunity. 2004; 21:669–679. [PubMed: 15539153]

Matsuda JL, Zhang Q, Ndonye R, Richardson SK, Howell AR, Gapin L. T-bet concomitantly controls migration, survival, and effector functions during the development of Valpha14i NKT cells. Blood. 2006; 107:2797–2805. [PubMed: 16357323]

McKinstry KK, Golech S, Lee WH, Huston G, Weng NP, Swain SL. Rapid default transition of CD4 T cell effectors to functional memory cells. J Exp Med. 2007; 204:2199–2211. [PubMed: 17724126]

O'Shea JJ, Paul WE. Mechanisms underlying lineage commitment and plasticity of helper CD4+ T cells. Science. 2010; 327:1098–1102. [PubMed: 20185720]

Odegard JM, Marks BR, DiPlacido LD, Poholek AC, Kono DH, Dong C, Flavell RA, Craft J. ICOS-dependent extrafollicular helper T cells elicit IgG production via IL-21 in systemic autoimmunity. J Exp Med. 2008; 205:2873–2886. [PubMed: 18981236]

Park JH, Yu Q, Erman B, Appelbaum JS, Montoya-Durango D, Grimes HL, Singer A. Suppression of IL7Ralpha transcription by IL-7 and other prosurvival cytokines: a novel mechanism for maximizing IL-7-dependent T cell survival. Immunity. 2004; 21:289–302. [PubMed: 15308108]

Pepper M, Linehan JL, Pagán AJ, Zell T, Dileepan T, Cleary PP, Jenkins MK. Different routes of bacterial infection induce long-lived TH1 memory cells and short-lived TH17 cells. Nat Immunol. 2010; 11:83–89. [PubMed: 19935657]

Poholek AC, Hansen K, Hernandez SG, Eto D, Chandele A, Weinstein JS, Dong X, Odegard JM, Kaech SM, Dent AL, et al. In vivo regulation of Bcl6 and T follicular helper cell development. J Immunol. 2010; 185:313–326. [PubMed: 20519643]

Polic B, Kunkel D, Scheffold A, Rajewsky K. How alpha beta T cells deal with induced TCR alpha ablation. Proc Natl Acad Sci USA. 2001; 98:8744–8749. [PubMed: 11447257]

Purton JF, Tan JT, Rubinstein MP, Kim DM, Sprent J, Surh CD. Antiviral CD4+ memory T cells are IL-15 dependent. J Exp Med. 2007; 204:951–961. [PubMed: 17420265]

Román E, Miller E, Harmsen A, Wiley J, Von Andrian UH, Huston G, Swain SL. CD4 effector T cell subsets in the response to influenza: heterogeneity, migration, and function. J Exp Med. 2002; 196:957–968. [PubMed: 12370257]

Swain SL, Hu H, Huston G. Class II-independent generation of CD4 memory T cells from effectors. Science. 1999; 286:1381–1383. [PubMed: 10558997]

R Development CoreTeam. R: A Language and Environment for Statistical Computing. Vienna, Austria: R Foundation for Statistical Computing; 2010.

Tokoyoda K, Zehentmeier S, Hegazy AN, Albrecht I, Grün JR, Löhning M, Radbruch A. Professional memory CD4+ T lymphocytes preferentially reside and rest in the bone marrow. Immunity. 2009; 30:721–730. [PubMed: 19427242]

Tripathi P, Mitchell TC, Finkelman F, Hildeman DA. Cutting Edge: Limiting amounts of IL-7 do not control contraction of CD4+ T cell responses. J Immunol. 2007; 178:4027–4031. [PubMed: 17371956]

Tripathi P, Kurtulus S, Wojciechowski S, Sholl A, Hoebe K, Morris SC, Finkelman FD, Grimes HL, Hildeman DA. STAT5 is critical to maintain effector CD8+ T cell responses. J Immunol. 2010; 185:2116–2124. [PubMed: 20644163]

Williams MA, Ravkov EV, Bevan MJ. Rapid culling of the CD4+ T cell repertoire in the transition from effector to memory. Immunity. 2008; 28:533–545. [PubMed: 18356084]

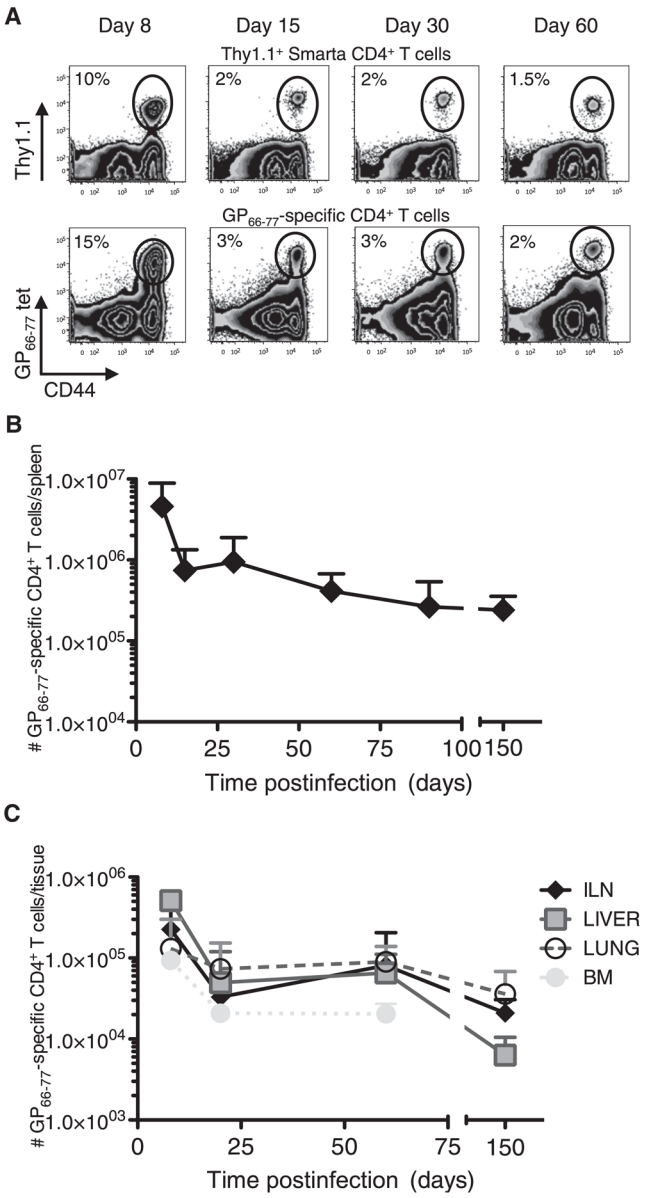

Figure 1. Kinetics of the LCMV-Specific $GP_{66–77}$ Stg and Polyclonal $CD4^+$ T Cell Responses

(A) Stg chimeric mice (top) or B6 mice (bottom) were infected with LCMV Armstrong, and 8, 15, 30, and 60 days p.i., splenocytes were analyzed for $Thy1.1^+$ or $GP_{66–77}$ $tetramer^+$ $CD4^+$ T cells.

(B and C) The number of $GP_{66–77}$-specific $CD4^+$ T cells in the spleen (B), inguinal lymph nodes, liver, lung, and bone marrow (C) was determined at various time points p.i. Cumulative numbers of tetramer and Stg TCR transgenic cells from 9–7 mice/time point from more than 20 independent experiments are graphed + SD. See also Figure S1.

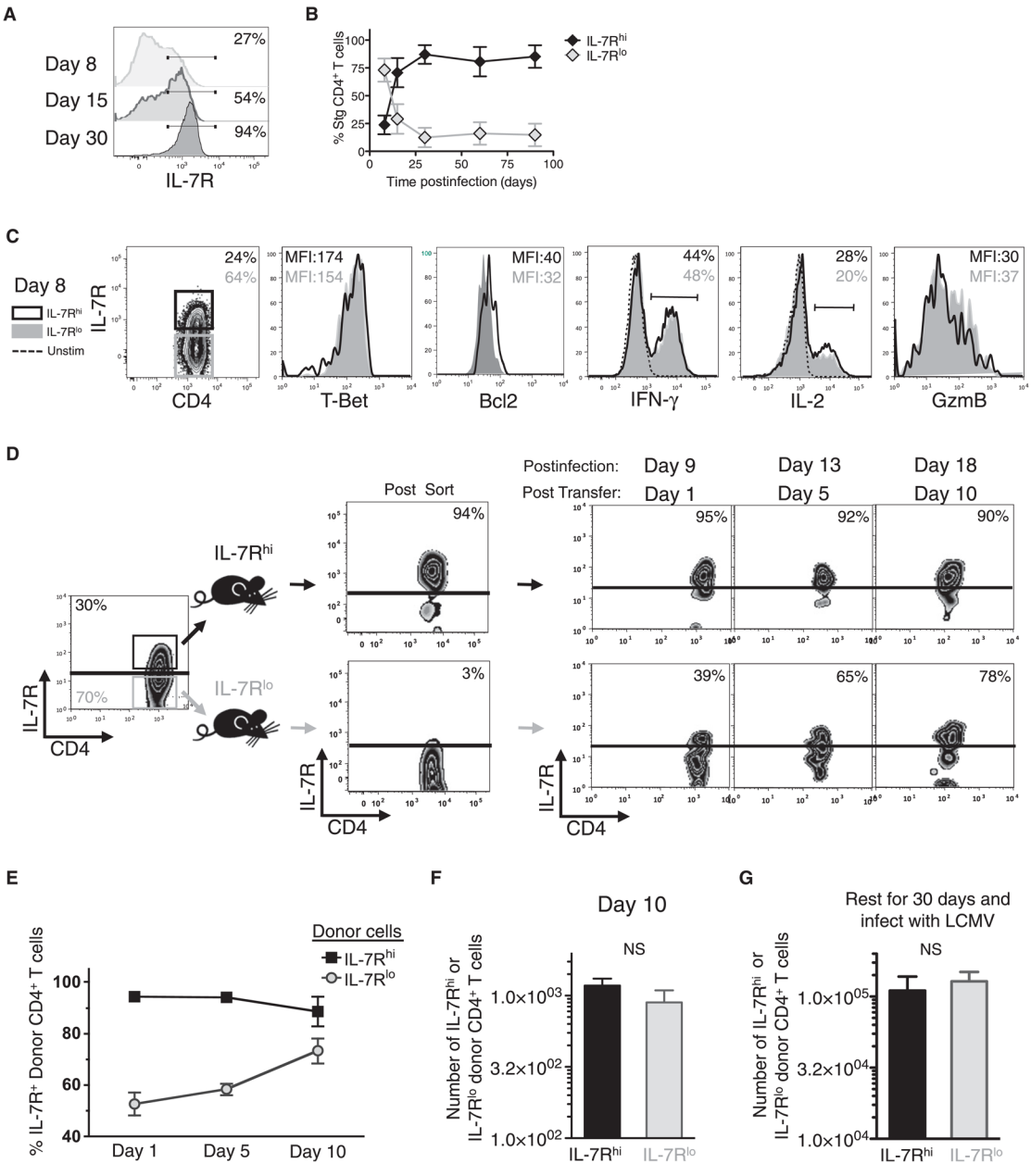

Figure 2. IL-7R Expression Does Not Mark Memory Precursor Effector CD4$^+$ T Cells

(A and B) Frequency of IL-7R on virus-specific CD4$^+$ T cells was determined at various time points p.i. and shown in histogram plots (A) and in line graph ± SD (B).

(C) Expression of the indicated proteins was compared between IL-7R^{hi} (black line) and IL-7R^{lo} (gray shaded) Stg CD4$^+$ T cells at day 8 p.i. and shown in overlapping histograms.

(D–F) IL-7R^{hi} (black) and IL-7R^{lo} (gray) Stg CD4$^+$ T cells were purified by FACS 8 days p.i. and equal numbers were transferred into infection-matched congenic recipients. Donor cells in the blood were analyzed for IL-7R expression over 10 days posttransfer and the frequency of IL-7R^{hi} donor T cells are shown in representative FACS plots (D) or cumulative line graph ± SD (E).

(F) Bar graph shows the absolute number of donor cells + SD recovered 10 days posttransfer.

(G) As in (D) above, except the donor IL-7R^{hi} and IL-7R^{lo} effector T cells were parked for 30 days in naive congenic recipients that were subsequently infected with LCMV. Seven days after secondary infection, the number of donor Stg CD4^{+} T cells in the spleen + SD was measured.

Data are cumulative of three independent experiments. NS, not statistically significant.

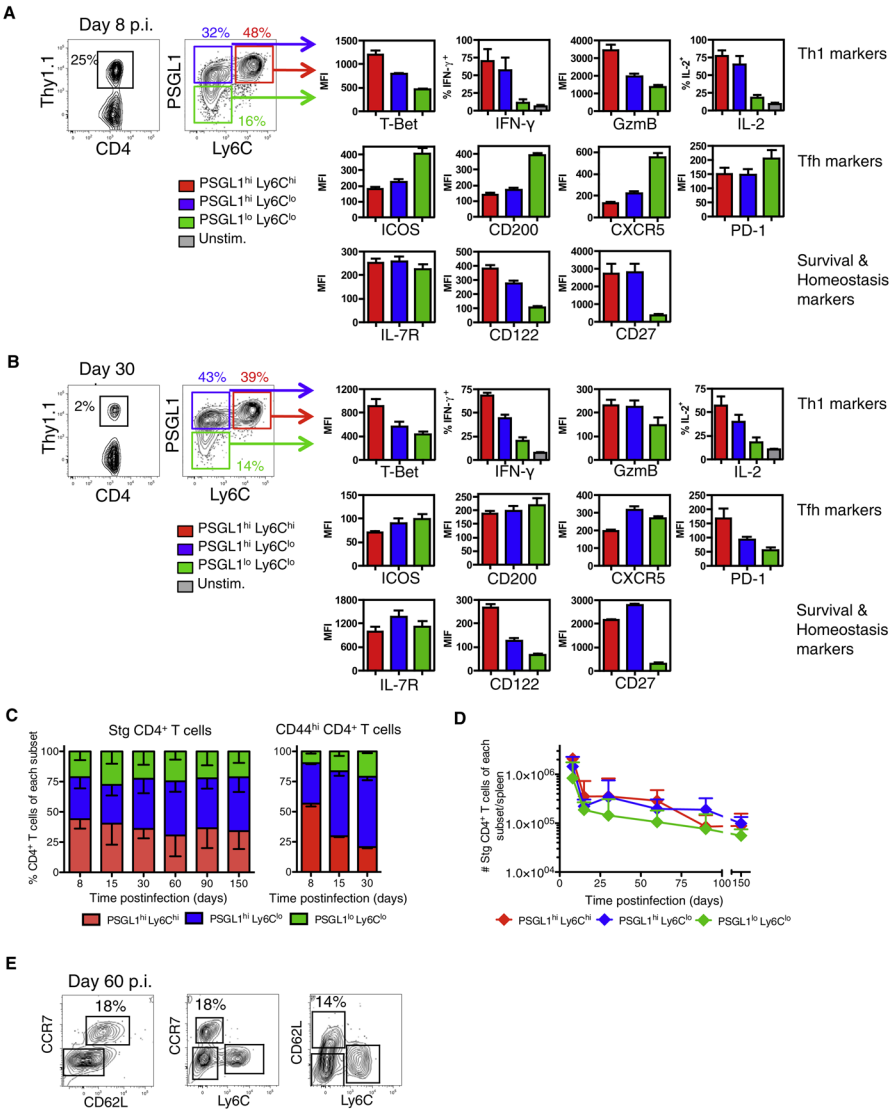

Figure 3. Formation of Distinct LCMV-Specific Effector CD4$^+$ T Cells Subsets

(A and B) Stg chimeric mice were infected with LCMV and 8 (A) or ~30 (B) days p.i. splenocytes were analyzed by flow cytometry for expression of the indicated proteins. PSGL1^{hi}Ly6C^{hi} (red), PSGL1^{hi}Ly6C^{lo} (blue), and PSGL1^{lo}Ly6C^{lo} (green) Stg CD4$^+$ T cells were gated and the average MFI + SD for the various proteins are shown in bar graphs. CD4$^+$ T cells were also stimulated with GP$_{61–80}$ peptide in vitro and the average frequency of IFN-γ$^+$ and IL-2$^+$ Stg T cells + SD are shown.

Data shown are representative of three independent experiments (n = 3 per group).

(C) Stacked bar graph of Stg CD4 T cells (left) or CD44^{hi} polyclonal CD4$^+$ T cells (right) – SD in each subset after LCMV infection.

(D) Total number of Stg CD4$^+$ T cells + SD of each subset during LCMV infection. Cumulative data from 9–37 mice/time point from more than 20 independent experiments are graphed.

(E) The expression of CD62L and CCR7 on Ly6C^{hi} and Ly6C^{lo} Stg CD4$^+$ T cells at day 60 p.i. is shown in FACS plots. See also Figure S2.

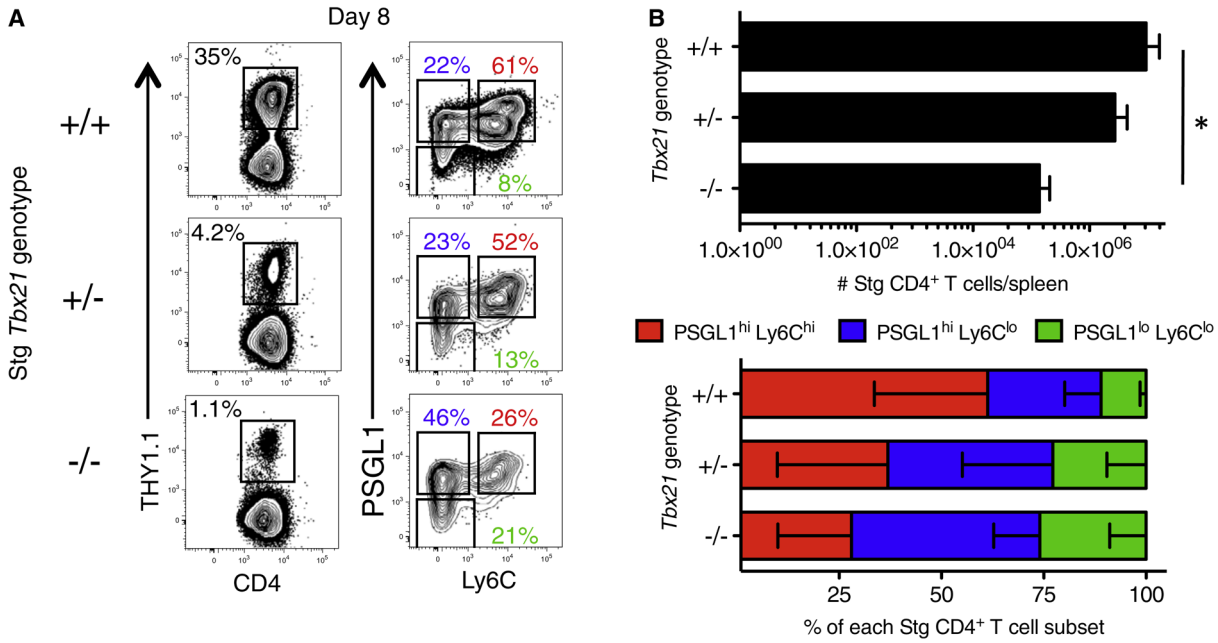

Figure 4. T-bet-Dependent Formation of Antiviral CD4$^+$ T Cell Subsets

1×10^4 *Tbx21*$^{+/+}$, *Tbx21*$^{+/-}$, or *Tbx21*$^{-/-}$ Stg CD4$^+$ T cells were adoptively transferred into three groups of mice and then infected with LCMV Armstrong. Eight days p.i. the frequency of Stg cells and expression of PSGL1 and Ly6C was analyzed. Representative examples in FACS plots (A) and cumulative numbers of donor Stg CD4$^+$ T cells + SD (B) and frequencies – SD of the different effector CD4$^+$ T cell subsets from three independent experiments. *$p < 0.05$.

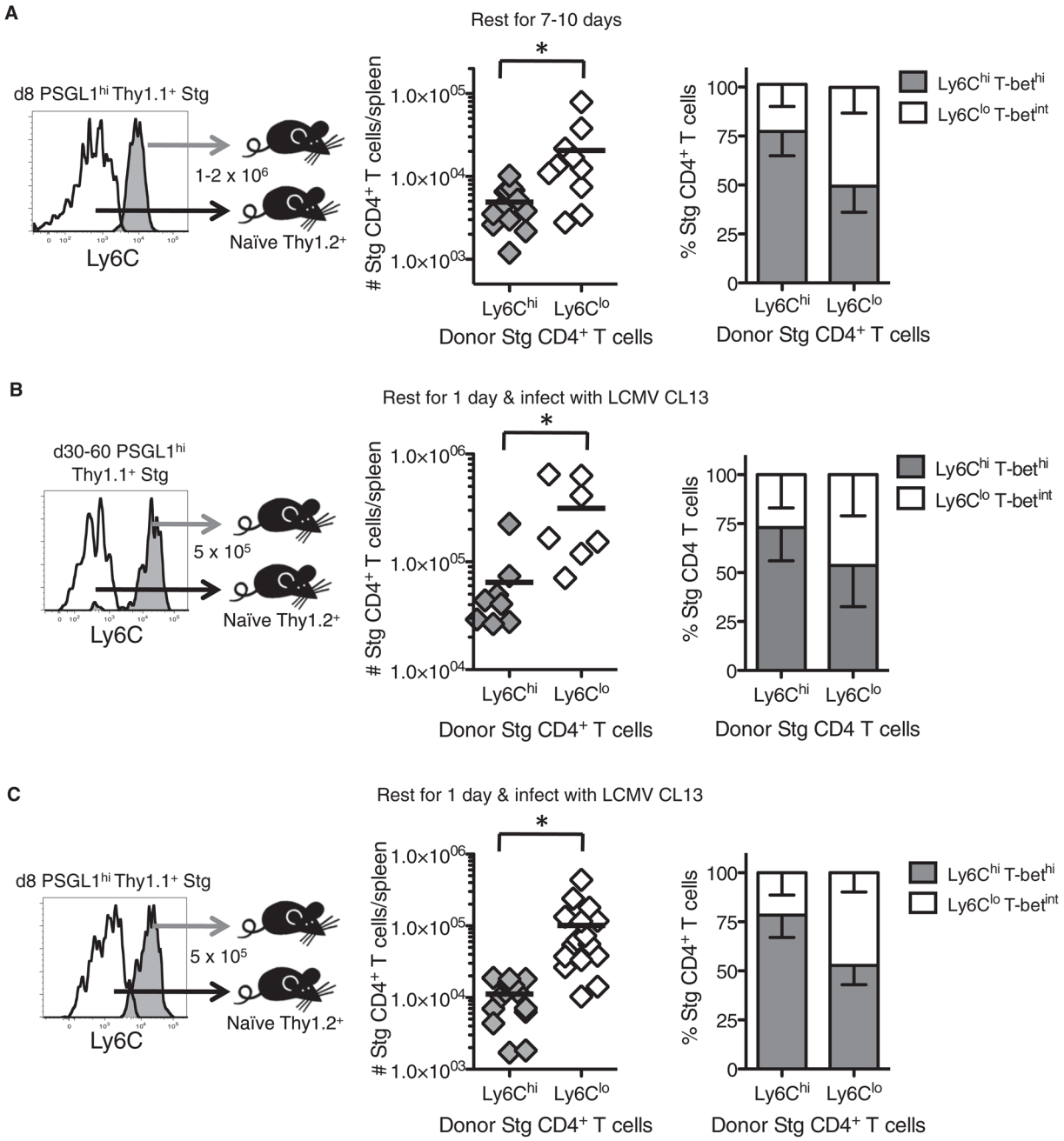

Figure 5. Enhanced Memory Cell Properties in PSGL1^{hi}Ly6C^{lo} Effector CD4$^+$ T Cells

(A) PSGL1^{hi}Ly6C^{hi} or PSGL1^{hi}Ly6C^{lo} Stg CD4$^+$ T cells were purified 8 days p.i. and adoptively transferred at equal numbers (~1.5 × 10^6) into naive congenic recipients. 7–10 days later, the number of donor Stg CD4$^+$ T cells remaining in the spleen and their phenotypes – SD were determined. Cumulative data from six independent experiments is shown; black line represents the mean.

(B and C) 5 × 10^5 PSGL1^{hi}Ly6C^{hi} or PSGL1^{hi}Ly6C^{lo} Stg CD4$^+$ T cells were purified 30–60 (B) or 8 (C) days p.i. and transferred into mice that were subsequently infected with LCMV clone 13. Six days later, the numbers of splenic donor Stg CD4$^+$ T cells and their

phenotypes were determined – SD. Cumulative data from three (B) or five (C) independent experiments are shown. *$p < 0.05$.

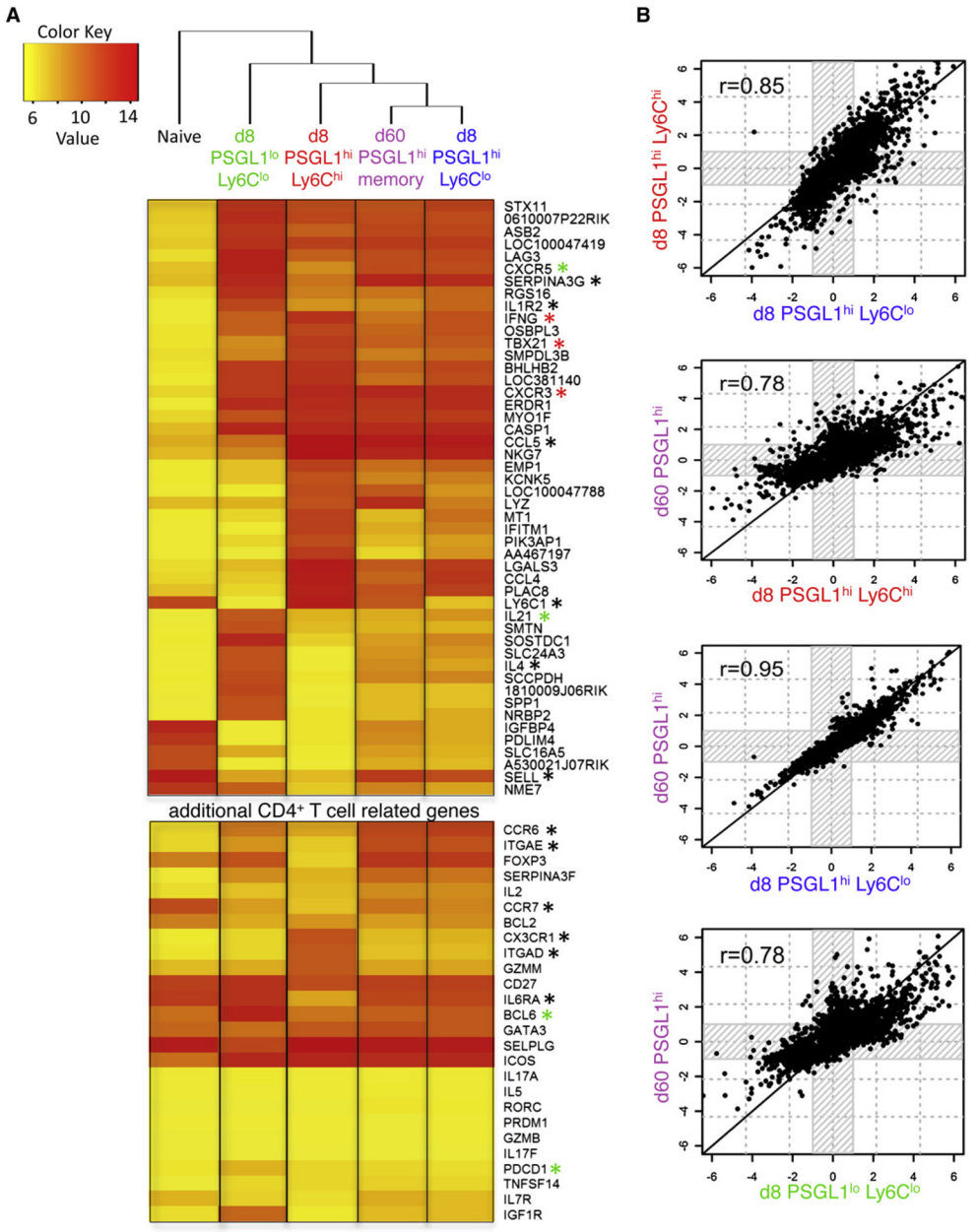

Figure 6. Gene Expression Profiles of PSGL1^{hi}Ly6C^{lo} Effector CD4^{+} T Cells and Memory CD4^{+} T Cells Are Highly Similar

Three independent Stg CD4^{+} T cell samples containing naive, day 8 PSGL1^{lo}Ly6C^{lo}, day 8 PSGL1^{hi}Ly6C^{hi}, day 8 PSGL1^{hi}Ly6C^{lo}, or day 60 PSGL1^{hi} memory CD4^{+} T cells were purified by FACS, and whole-genome mRNA expression profiles were characterized with Illumina microarrays. See also Table S1.

(A) Clustering analysis and heatmap of expression values showing the $\log_2$ transformed expression intensity of any gene with a 32-fold change or higher over naive ($q < 0.0001$). Genes marked by an asterisk are mentioned in the Results or Discussion.

(B) The overall similarity in gene expression between the different effector and memory CD4^{+} T cell samples was examined, in a pairwise manner, by identifying all the genes that were differentially expressed in any sample relative to naive CD4^{+} T cells (greater than 2-

fold change and $q < 0.05$) and then plotting their relative intensities in each respective sample compared to the naive population.

Table 1

Differentially Expressed Genes in PSGL1^{hi}Ly6C^{hi} Compared to PSGL1^{hi}Ly6C^{lo} Effector CD4^{+} T Cell Subsets

	PSGL1^{hi}Ly6C^{hi} Compared to PSGL1^{hi}Ly6C^{lo}	**PSGL1^{hi}Ly6C^{hi} Compared to Naive**	**PSGL1^{hi}Ly6C^{lo} Compared to Naive**
Ly6c1	78.19	4.80	−15.26
Cx3cr1	8.70	22.95	2.64
Itgad	7.08	18.35	2.59
Il18rap	5.38	23.31	4.34
Gzmm	4.79	8.74	1.77
Irak3	4.36	7.93	1.82
Ifng	4.36	95.63	24.03
Ccr5	3.72	18.70	5.03
Tbx21	3.14	58.36	18.62
Il12rb2	2.67	3.45	1.29
Il21	−1.49	4.30	6.39
Bcl6	−1.74	−1.10	1.59
Cd200	−1.99	−1.43	1.40
Il2	−2.62	2.30	6.03
Serpina3f	−3.46	3.97	13.12
Ccr7	−3.88	−12.96	−3.34
Cxcr5	−4.31	3.25	13.59
Il4	−6.43	1.08	5.93
Il6ra	−6.84	−10.85	−1.59
Serpina3g	−7.72	4.44	34.24
Ccr6	−8.03	2.56	20.55
Igf1r	−9.14	−3.81	2.40
Folr4	−10.06	−5.70	1.59
Cd81	−13.00	−3.10	4.19
Sell	−10.82	−7.84	1.38
Nt5e	−11.85	−67.43	−5.69
Cd83	−14.15	−1.58	8.96
Itgae	−14.46	1.17	16.87
Nrn1	−18.36	−1.87	9.80
Foxp3	−29.56	−4.37	4.87

A selective list of differentially expressed genes between PSGL1^{hi}Ly6C^{hi} and PSGL1^{hi}Ly6C^{lo} effector CD4^{+} T cell subsets based on fold change as determined with GeneSpring GX11. The fold change values of PSGL1^{hi}Ly6C^{hi} compared to PSGL1^{hi}Ly6C^{lo} (left), PSGL1^{hi}Ly6C^{hi} compared to naive (middle), and PSGL1^{hi}Ly6C^{lo} compared to naive (right) are shown. See also Table S2.